Pennec, Y.; Rouhani, BD.; Li, C.; Escalante Fernández, JM.; Martínez Abietar, AJ.; Benchabane, S.; Laude, V.... (2011). Band gaps and cavity modes in dual phononic and photonic strip waveguides. AIP Advances. 1(4):41901-41908. doi:10.1063/1.3675799.

Band Gaps and Cavity Modes in Dual Phononic and Photonic Strip Waveguides

Y. Pennec[1], B. Djafari Rouhani[1], C. Li[1], J. M. Escalante[2], A. Martinez[2], S. Benchabane[3],

V. Laude[3], N. Papanikolaou[4]

[1]*Institut d'Electronique, Microélectronique et Nanotechnologie, UMR CNRS 8520*
Université Lille 1, Villeneuve d'Ascq, France
[2] *Nanophotonics Technology Center, Universidad Politécnica de Valencia, Spain*
[3] *Institut FEMTO-ST, Université de Franche Comté and CNRS, Besançon, France*
[4] *Institute of Microelectronic, NCSR, Athena, Greece*

We discuss theoretically the simultaneous existence of phoxonic, i.e., dual phononic and photonic, band gaps in a periodic silicon strip waveguide. The unit-cell of this one-dimensional waveguide contains a hole in the middle and two symmetric stubs on the sides. Indeed, stubs and holes are respectively favorable for creating a phononic and a photonic band gap. Appropriate geometrical parameters allow us to obtain a complete phononic gap together with a photonic gap of a given polarization and symmetry. The insertion of a cavity inside the perfect structure provides simultaneous confinement of acoustic and optical modes suitable to enhance the phonon-photon interaction.

I. INTRODUCTION

Phononic [1, 2] and photonic crystals [3, 4] have both received a great deal of attention during the last two decades. These infinite 2D periodic structures, constituted by a periodical repetition of inclusions in a matrix background, have opened up new features for controlling sound and light, leading to the proposition of many novel acoustic [5] and optical [6] devices. The interest on these structures is partly based on their ability to exhibit absolute band gaps and localized modes associated with defects forming waveguides and cavities. The existence of band gaps and confined modes has especially been investigated in photonic crystal slabs [7, 8] and more recently in phononic slabs [9-13], in particular in view of the technological realization of integrated structures for electronics and telecommunications. Another structure, widely used in photonics, is constituted by a 1D narrow strip waveguide where for instance a silicon waveguide is periodically drilled with holes. Such 1D photonic crystals are recognized for their ability to manipulate light and could become promising in building interconnects for the integration of optical functions on a chip [14-16]. However, few studies have been dealt with the phononic properties of periodic strip waveguides [17].

Following recent advances in nanotechnology fabrication, the simultaneous control of phonons and photons in the same structure with the aim of enhancing their interaction has received a great deal of attention during the last few years. Dual phononic-photonic (also called Phoxonic) structures hold promises for the simultaneous confinement and tailoring of sound and light waves, with potential applications to acousto-optical devices and highly controllable phonon-photon interactions. The existence of dual photonic and phononic band gaps has been investigated first in 2D infinite crystal for air holes drilled in silicon [18, 19], lithium niobate [20] or sapphire matrices [21]. Similar demonstrations have been performed in 2.5D finite silicon crystal slabs with inclusions composed of holes [22. 23], pillars [24] or "snow-flake" structures [25]. The periodic slab is also used to design linear [25-27] and cavity defects [28, 29] in which the confinement of both excitations or the existence of slow waves is expected to strongly enhance their interaction.

The enhancement of photon-phonon interaction has been also investigated in 1D strip waveguides. Eichenfield et al. [30. 31] proposed a 1D patterned optomechanical nanobeam made up of a periodic array of rectangular shaped holes in a straight waveguide. Optically, the structure has a complete photonic band gap, but not a mechanical gap. This makes the structure susceptible of mechanical losses, especially when a cavity is inserted. It remains that, up to now, the theoretical demonstration of a complete absolute phononic and photonic band gap in 1D nanobeam structure is still missing.

The aim of this paper is to investigate both the acoustic and optical band structures, and in particular the existence of dual phononic-photonic band gaps, in a model silicon strip waveguide in which each unit cell contains one hole in the middle and two symmetric stubs on the sides. The geometry of the structure is motivated by the fact that the stubs and holes are respectively favorable for the opening of phononic and photonic gaps. In section II, we present the methods of calculations we have used, namely the finite-element (FE) method for dispersion curves and the finite difference time domain (FDTD) method for transmission spectra. In section III, we shall discuss the existence and evolution of these gaps as a function of the geometrical parameters in the structure. Then, we show in section IV the possibility of simultaneous confinement of phonons and photons when a defect cavity is inserted inside the strip waveguide. Conclusions are presented in section V.

II. MODEL AND METHOD OF CALCULATION

Figure 1(a) depicts a schematic view of the periodical silicon strip waveguide made up of a straight waveguide combined with symmetric stubs grafted on each side and circular holes drilled in the middle. The choice of silicon is motivated both by its technological interest in electronics and telecommunications and the fact that silicon strips are able to guide optical waves. Silicon is taken as a cubic material with elastic constants C_{11}=165.7 GPa, C_{12}=63.9 GPa, C_{44}=79.62 GPa, and mass density ρ=2331 kg/m^3. Silicon is optically isotropic with a refractive index of 3.47. In Figure 1a, the z axis is

directed along the strip waveguide and defines the propagation direction. The y axis is chosen perpendicular to the strip waveguide and parallel to the hole axis. The lattice period Λ can be considered as the unit of length. Then, the geometrical parameters involved in the structure are the width of the waveguide $w=\Lambda$, the length w_e and width w_i of the symmetric stubs, the thickness h of the strip and the diameter d=2r of the air hole. Figure 1(b) shows the elementary unit cell. Bloch-Floquet periodic boundary conditions are applied on the sides of the unit cell that are orthogonal to axis z. In phononic calculations, stress-free boundary conditions are applied on all others surfaces of the strips, since elastic waves cannot propagate in air. In photonic calculations, one has to consider a large volume of air around the strip and artificial periodic boundary conditions are applied in the x and y directions. The air thickness in each direction is taken as five times the lattice parameter Λ in order to ensure convergence of the dispersion diagram under the light cone. The guided modes and the associated band gaps are searched under the light cone because above the light line the modes radiate into the vacuum. However, due to the small imperfections in the actual fabrication of samples, some guided modes may couple to the leaky waves above the light line and become lossy. The structure shown in Fig. 1a possesses two symmetry planes, Π (normal to y) and Π' (normal to x), so that all branches in the dispersion curves can be labeled according to their symmetry (odd or even) with respect to these planes.

In all band diagrams presented in this paper, frequencies are given in dimensionless units $\Omega=\omega\Lambda/2\pi c$, where c is either the velocity of light in vacuum for electromagnetic waves or the transverse velocity of sound in silicon (c_t=5844m/s) for elastic waves.

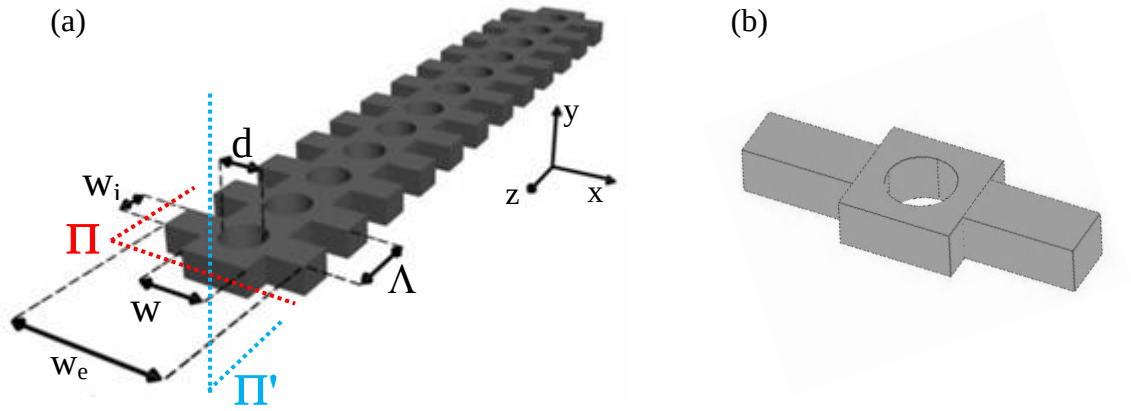

Fig. 1: (a) Schematic view of the periodic silicon strip waveguide. (b) Representation of the unit cell which contains one hole in the middle of the waveguide and two symmetric stubs on each side.

III. PHONONIC/PHOTONIC BAND GAPS

The purpose of this section is to find dual phononic and photonic band gaps in the structured nanobeam of Fig. 1. Up to now, strip waveguides have been mainly studied in photonics where the possibility of band gaps was demonstrated both in straight waveguides containing air holes [14] and in stubbed waveguides [16]. Regarding elastic waves, Hsu et al. [17] discussed the formation of the band gaps in two phononic strip waveguides, cut from a phononic crystal plate. Eichenfield et al. [30, 31] studied an optomechanical straight nanowire containing periodic rectangular holes supporting photonic band gaps but no phononic band gaps. The demonstration of dual phononic-photonic gaps in strip waveguides is therefore still missing and is the subject of the following investigation. The insertion of periodical holes in the waveguide is actually sufficient to create a photonic band gap while the stubbed waveguide supports phononic band gaps. For this reason, we propose to study the geometry of Fig. 1 where each unit cell contains a combination of a hole and two symmetric stubs. By varying the geometrical parameters, we shall show that the phononic band gap is mainly sensitive to the size of the stubs whereas it is practically independent of the holes diameter. On the other hand, the hole diameter plays the most significant role in the photonic dispersion curves.

Figure 2a represents the phononic dispersion curve in the Brillouin zone for geometrical parameters w_e/Λ=3.0, w_i/Λ=0.5, h/Λ=0.44, and r/Λ=0.3. As expected, the band diagram of the nanobeam shows four acoustic branches starting from the Γ point. At higher frequencies, the structure displays a complete phononic band gap in the reduced frequency range [0.306, 0.355]. In Figs. 2b to 2e, we show the evolution of this gap as a function of the geometrical parameters of the structure.

Figure 2b represents the band gap map for a variation of the full length w_e/Λ of the symmetric stubs. The gap is opened in a large range of values of w_e, from 2.7Λ to 3.7Λ, with a decrease in the central frequency of the gap as w_e increases. In Fig. 2c, one can see that in order to open the gap the width of the stubs has to be larger than 0.3Λ. For a width $w_i \geq 0.5\Lambda$, the width and frequency of the gap remain almost constant. These trends support the fact that the geometrical parameters of the stub affect very significantly the formation of the phononic gap. The evolution of the band gaps as a function of the thickness of the strip is sketched in figure 2d. As in the case of a phononic slab drilled with holes [9], the thickness has to be close to half the lattice parameter. Finally, the band gap is not very sensitive to the radius of the holes (Fig. 2e) and remains open for any radius ranging from 0 to 0.45Λ.

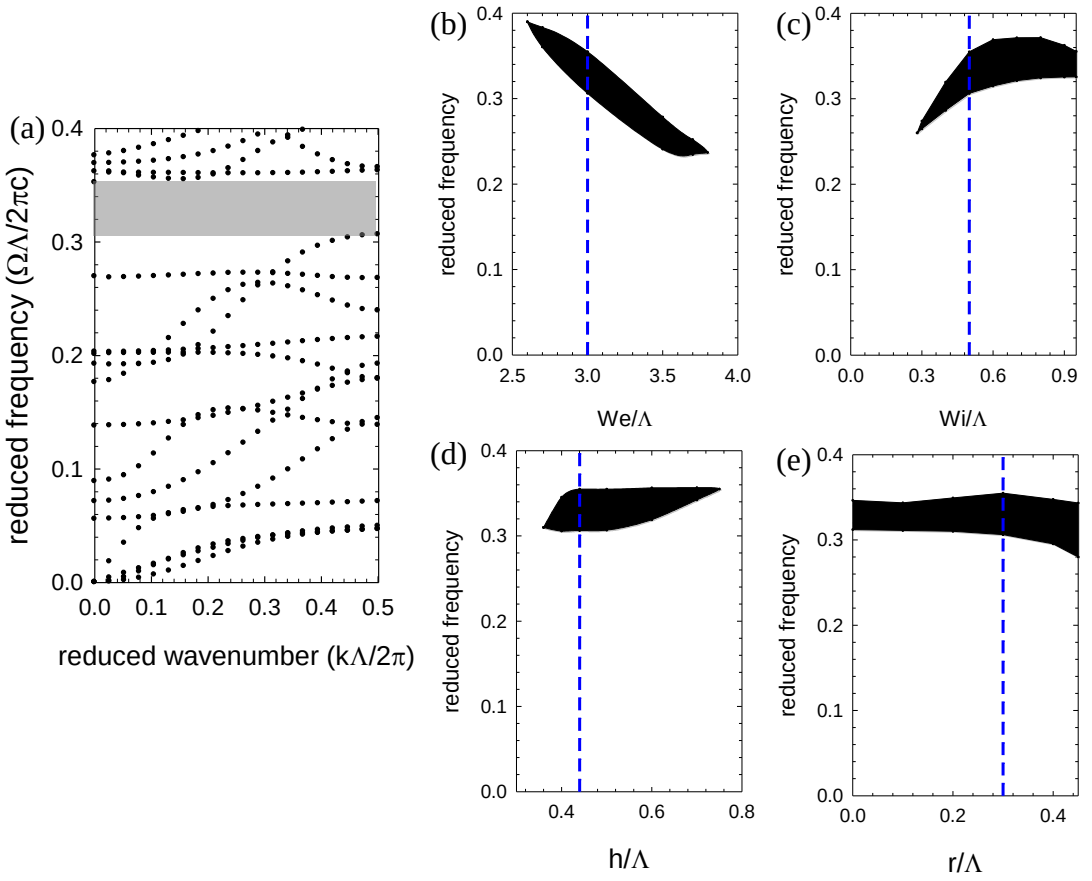

Figure 2: (a) Phononic dispersion curve for the stubbed waveguide of figure 1 with parameters w_e/Λ=3.0, w_i/Λ=0.5, h/Λ=0.44, and r/Λ=0.3. (b, c, d and e) Evolution of band gap edges as a function of each geometrical parameter, the others being kept constant: (b) w_e/Λ, (c) w_i/Λ, (d) h/Λ and (e) r/Λ. The vertical blue dashed lines give the values of the parameters used in the calculation of the dispersion curves presented in (a).

Keeping the geometrical parameters of the stubs suitable for the opening of the phononic band gap (w_i/Λ=0.5 and w_e/Λ=3.0) and choosing a thickness h/Λ=0.44, we study in Fig. 3 the variations of the photonic dispersion curves as a function of the hole radius r. Band diagrams are presented for r/Λ=0.0, 0.3, and 0.45. By increasing the hole radius from zero, the branches under the light cone, which represent guided modes of the strip, move upwards. Therefore, the number of branches decreases in a sufficiently large frequency range corresponding to Λ/λ smaller than 0.35. Although there is no absolute photonic band gap for an arbitrary polarization of light, one can search for band gaps among those branches which are of the same symmetry with respect to the symmetry planes Π' and Π of the structure (see Fig.1).

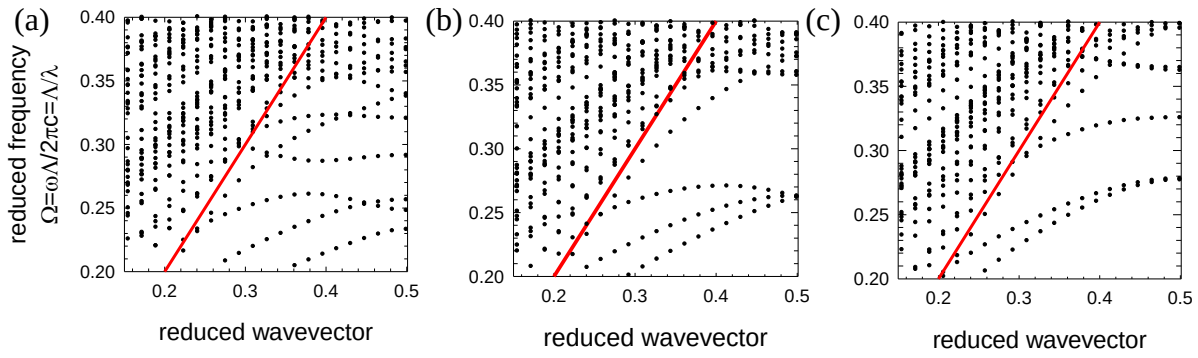

Figure 3: Photonic dispersion curves for the same parameters (h/Λ=0.44, w_i/Λ=0.5 and w_e/Λ=3.0) as in figure 2a but for three different radii: (a) r/Λ=0.0, (b) r/Λ=0.3 and (c) r/Λ=0.45. In figure b, modes are labeled as odd (o) or even (e) with respect to the symmetry planes Π' and Π of the structure. The reduced frequency is given by Ω=ωΛ/2πc=Λ/λ, where c is the velocity of light in vacuum.

This symmetry analysis has been conducted from the calculation of the electric and magnetic fields associated with the branches in Fig. 3b. For the lowest four branches, this assignment is supported by the maps (Fig. 4) of the x component of the electric field at the reduced wavenumber kΛ/2π=0.414. The first and third branches have the same symmetry oe, namely odd with respect to Π' and even with respect to Π. The second and fourth branches are respectively ee and eo. Therefore, there is a wide photonic gap with oe symmetry in the frequency range [0.270, 0.337] between branches 1 and 3. An incident light with such symmetry can only excite the latter branches and therefore cannot propagate in the range of the frequency range of the gap.

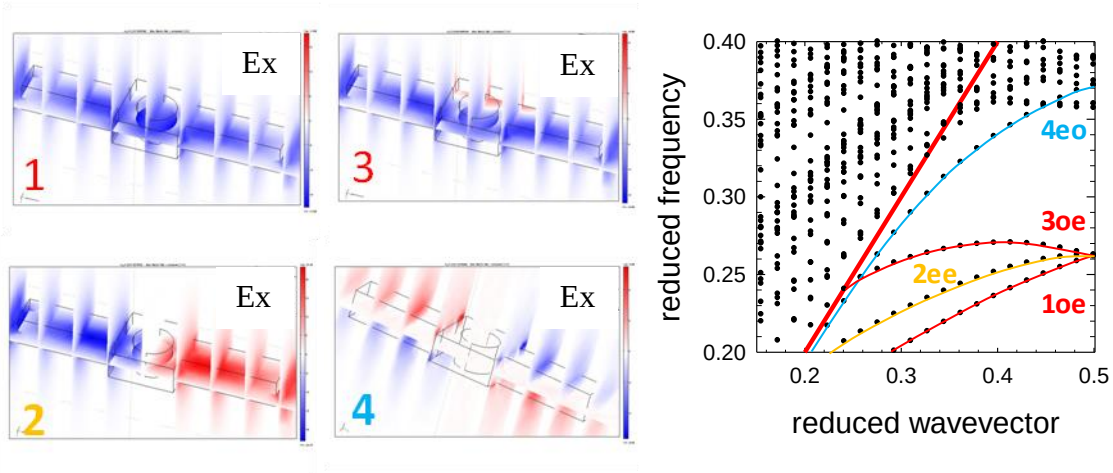

Figure 4: Map of the x component of the electric field for the lowest four modes in Fig. 3b at the reduced wavenumber kΛ/2π=0.414.

IV. PHONONIC/PHOTONIC CAVITY MODE

The strip waveguide defined in the previous section with the geometrical parameters w_e/Λ=3.0, w_i/Λ=0.5, h/Λ=0.44, and r/Λ=0.3, presents a full phononic band gap and a photonic band gap of a given symmetry. The aim of this section is to show the possibility of simultaneous confinement of phonons and photons in a cavity (Fig. 5a) inserted in the strip waveguide. The cavity is created by simply changing the distance between two neighboring unit cells along the z direction, as depicted in figure 5a. The width of the cavity is characterized by the elongation parameter Δ, i.e. Δ=0 when the crystal is perfect.

We calculate the phononic band structure by FEM using a super-cell constituted of the cavity surrounded by three normal cells on each side (Fig.5a). The separation between two neighboring cavities is sufficient to avoid interaction between them. Dispersion curves are shown in Fig. 5b for a cavity of length Δ/Λ=0.4. The white area representing the band gap is delimited by the propagating bands (grey areas) of the perfect structure. The insertion of a defect cavity introduces new modes in the band gap which correspond to localized modes inside the cavity. These branches move downwards and their number increases as the size of the cavity increases.

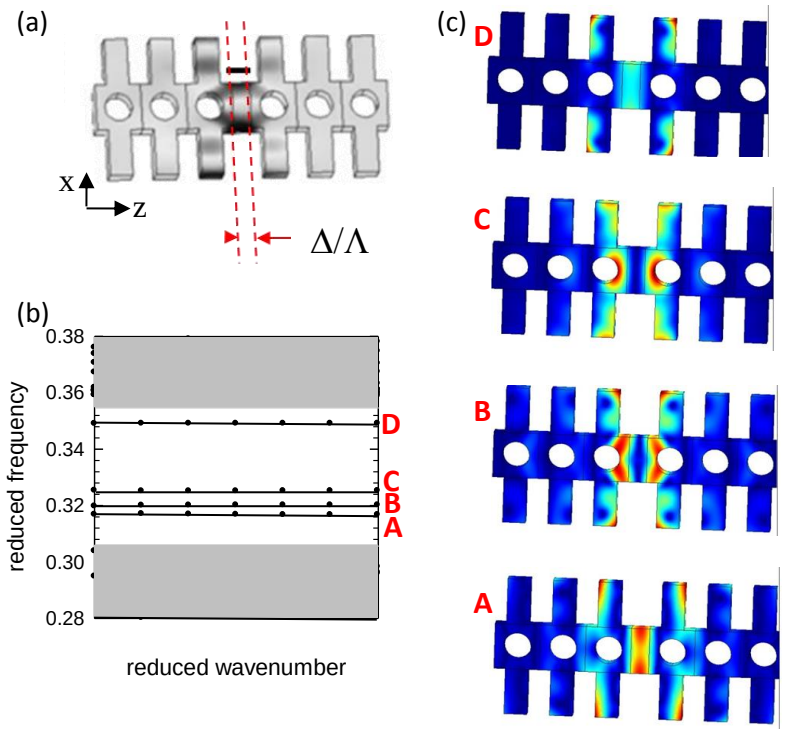

Figure 5: (a) Geometry of the cavity defined by the length Δ. (b) Phononic dispersion curves along the ΓX direction of the strip waveguide for a cavity of length Δ/Λ=0.4. (c) Modulus of the displacement field calculated at the points A, B, C, and D of the dispersion curves.

The flatness of the branches is a signature of their confinement inside the cavity. To support this statement, we display in Fig. 5c the modulus of the displacement field for the modes labeled A, B, C and D in Fig. 5b. Depending on the considered mode, the displacement field is essentially localized inside the defect cavity and inside the first stubs surrounding the cavity.

On the photonic side, dispersion curves obtained with the super-cell method are not easily interpreted. This is due to the many foldings of the dispersion curves in the reduced Brillouin zone associated to the super-cell, giving rise to a large number of branches above the light line. In this case, it is more efficient to calculate the transmission coefficient when an incident wave is launched towards the strip and to explore the possibility of a wave being confined inside the cavity. This calculation is performed with the help of a homemade three-dimensional finite difference time domain (3D-FDTD) code. The model is composed of a 3D-box made up of the silicon strip waveguide embedded in air with perfect matching layers (PML) conditions applied at all boundaries. The structure (figure 6a) is constituted by (i) an incoming straight waveguide where light is injected; (ii) the periodic waveguide composed of eight unit cells and the central cavity, and (iii) an outgoing straight waveguide where the output signal is detected. Space is discretized in both three directions using a mesh interval equal to $\Lambda/20$. The equations of motion are solved with a time integration $\Delta t = \Delta x/(4c)$, where c is the velocity of light in vacuum, and a number of time step equal to 2^{22}, which is the necessary time for a good convergence of the numerical calculation.

The injected pulse is generated at the left side of the 3D-box by a current source appropriate to create the optical wave with the desired symmetry which in our case should be respectively odd and even with respect to the symmetry planes Π' and Π. The transmitted signal, probed at the end of the right part of the strip waveguide, is recorded as a function of time and finally Fourier transformed to obtain the transmitted amplitude of the fields versus reduced frequency.

Figure 6b shows the amplitude of the transmitted electric and magnetic fields. In the presence of the cavity, a sharp peak appears inside the band gap at the reduced frequency 0.3172. This peak is magnified in the right part of figure 6b. In the inset of the figure, we show the evolution of the frequency of the peak as a function of the length Δ/Λ of the cavity. This frequency decreases by increasing Δ, so the position of the resonant mode can be tuned inside the gap.

To give a better view about the confinement of the resonant mode, we show in Fig.7 the maps of the electric and magnetic fields for a monochromatic excitation at the reduced frequency of the peak (0.3172).

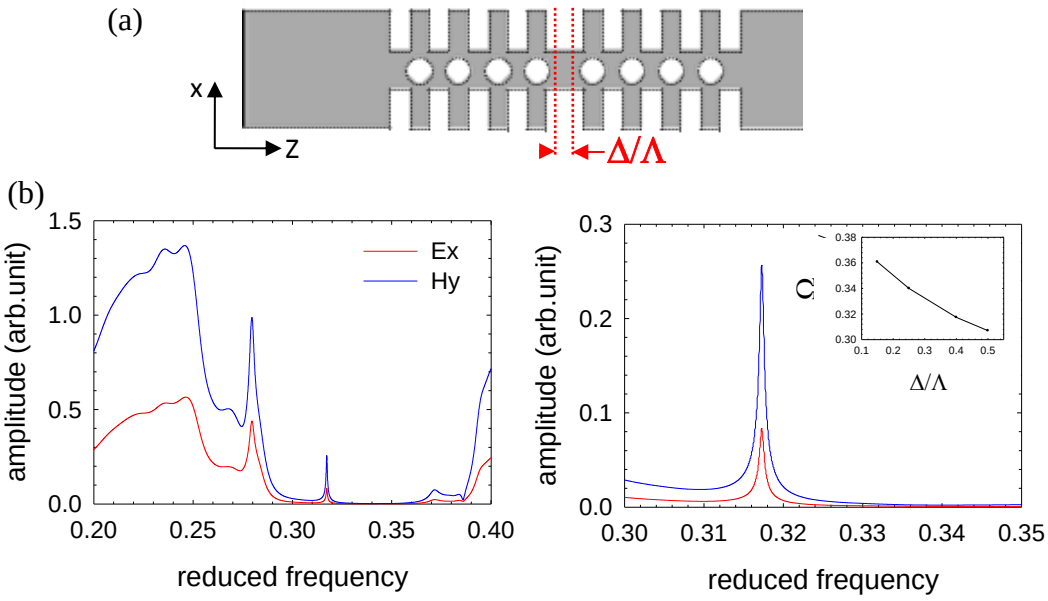

Figure 6: (a) Schematic view of the (x,z) section of the structure used for the 3D-FDTD calculation of the transmission, with Δ/Λ=0.4. (b) Left: Transmission coefficients for the electric and magnetic fields displaying a resonant peak inside the gap. Right: Magnification of the resonant peak. The inset shows the evolution of the peak frequency as a function of Δ.

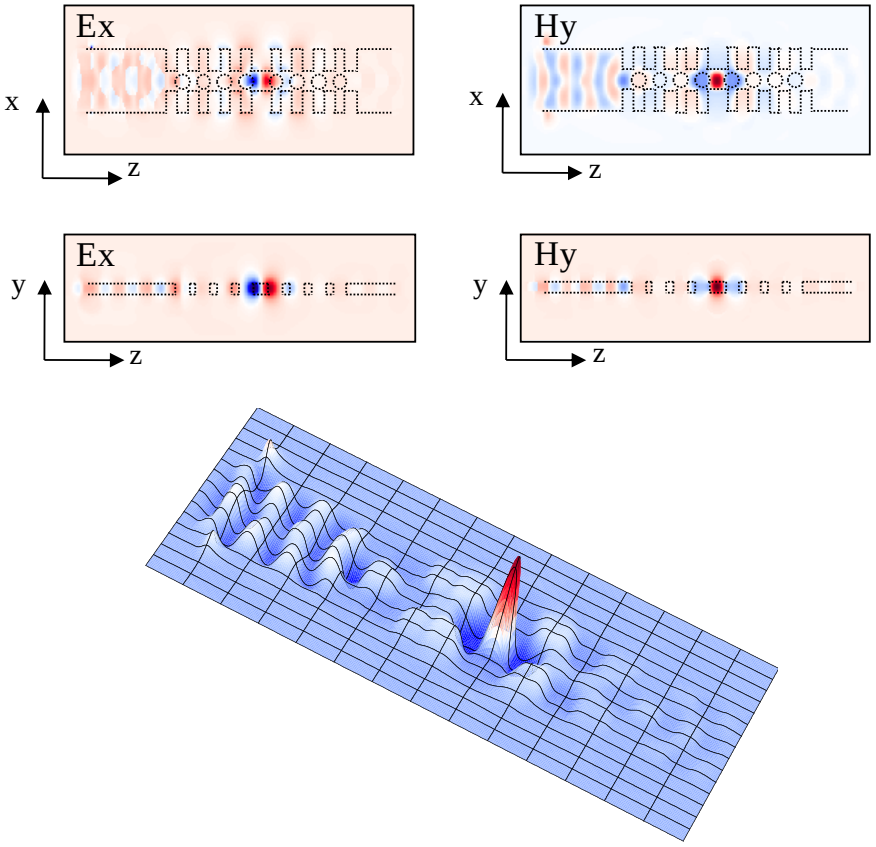

Figure 7: (a) Maps of the electric and magnetic fields in the strip waveguide structure containing a cavity with length Δ/Λ=0.4 at the monochromatic frequency 0.3172. (b) 3D map of the magnetic field.

As a conclusion, the introduction of a cavity of length Δ/Λ=0.4 in the strip waveguide allows us to obtain simultaneous confinement of both acoustic and optical waves inside the cavity. A look at the maps of the confined modes show that the most significant overlap between both waves, which is a necessary condition to enhance their interaction, is achieved with the acoustic cavity mode named (A) in figure 5c.

It is worthwhile noticing that in the above calculations the geometrical parameters were defined in comparison with the period Λ of the structure taken as the unit of length. Therefore, the phenomena described in this paper can be produced in different frequency ranges depending on the actual value of Λ. If the working optical frequency is chosen to be at the telecommunication wavelength of 1550 nm, then the geometrical parameters become Λ=500 nm, w_e=1500 nm, w_i=250 nm, h=220 nm, r=150 nm and Δ=200 nm. These parameters make the periodic strip waveguide technologically feasible. In this case, the acoustic mode (A) of Fig. 5c has a resonance frequency of 3.7 GHz.

V. CONCLUSION

In this work, we have investigated theoretically a periodical silicon nanowire made up of a straight waveguide combined with symmetric stubs grafted on each side and circular holes drilled in the middle. Appropriate choices of the geometrical parameters have allowed us to obtain a complete phononic gap together with a photonic gap of a given polarization and symmetry. We have shown that stubs and holes are respectively favorable for creating a phononic and a photonic band gap. We have then investigated the possibility of confining modes inside a defect cavity inserted in the phoxonic strip waveguide. Such a cavity can simultaneously confine phonons and photons, providing with an overlap of their fields which can enhance their interaction. Finally, we discussed actual values of the geometrical parameters, compatible with technological fabrication constraints, in order to find the photonic cavity mode in the range of telecommunication wavelengths, with the acoustic frequencies falling in the gigahertz regime.

Acknowledgments: This work was supported by the European Commission Seventh Framework Programs (FP7) under the FET-Open project TAILPHOX N° 233883.

References:

1. M.S. Kushwaha, P. Halevi, L. Dobrzynski and B. Djafari-Rouhani, “Acoustic band structure of periodic elastic composites”, Phys. Rev. Lett. **71**, 2022-2025 (1993).
2. M.M. Sigalas and E.N. Economou, “Band structure of elastic waves in two dimensional systems”, Solid State Commun. **86**, 141 (1993).
3. E. Yablonovitch, "Photonic band-gap structures", J. Opt. Soc. Am. B **10**, 283 (1993).
4. J. Joannopoulos, P. Villeneuve, S. Fan, S. Nature **383**, 699 (1996).
5. Y. Pennec, J. O. Vasseur, B. Djafari-Rouhani, L. Dobrzyński and, P. A. Deymier, ‘Two-dimensional phononic crystals: Examples and applications’, Surface Science Reports **65**, 229 (2010).
6. S. Fan, P. Villeneuve, J. Joannopoulos, and H. Haus, “Channel drop filters in a photonic crystal”, “Channel drop filters in a photonic crystal”, Opt. Express **3**, 4 (1998).
7. S. Shi, C. Chen, and D. W. Prather, “Plane-wave expansion method for calculating band structure of photonic crystal slabs with perfectly matched layers”, J. Opt. Soc. Am. A **21**, 1769 (2004).
8. S. G. Johnson, S. Fan, P. R. Villeneuve, J. D. Joannopoulos, and L. A. Kolodziejski, “Guided modes in photonic crystal slabs”, Phys. Rev. B **60**, 5751 (1999).
9. A. Khelif, B. Aoubiza, S. Mohammadi, A. Adibi, and V. Laude, “Complete band gaps in two-dimensional phononic crystal slabs” Phys. Rev. E **74**, 046610 , (2006).
10. C. Charles, B. Bonello, and F. Gannot, “Propagation of guided elastic waves in 2D phononic crystals”, Ultrasonics **44**, 1209(E) (2006).
11. J.O. Vasseur, P.A. Deymier, B. Djafari-Rouhani, Y. Pennec and A.C. Hladky-Hennion, “Absolute forbidden bands and waveguiding in two-dimensional phononic crystal plates”, Phys. Rev. B **77**, 085415 (2008).
12. Y. Pennec, B. Djafari-Rouhani, H. Larabi, J.O. Vasseur and A.C. Hladky-Hennion, “Low-frequency gaps in a phononic crystal constituted of cylindrical dots deposited on a thin homogeneous plate”, Phys. Rev. B **78**, 104105 (2008).
13. T.T. Wu, Z.G. Huang, T.-C. Tsai, and T.C. Wu, Appl. Phys. Lett. **93**, 111902 (2008).
14. J. S. Foresi, P. R. Villeneuve, J. Ferrera, E. R. Thoen, G. Steinmeyer, S. Fan, J. D. Joannopoulos, L. C. Kimerling, Henry I. Smith and E. P. Ippen, Photonic-bandgap microcavities in optical waveguides”, Nature **390**, 143, 1997.
15. Md Zain, Ahmad R; Johnson, Nigel P; Sorel, Marc; De La Rue, Richard M, “Ultra high quality factor one dimensional photonic crystal/photonic wire micro-cavities in silicon-on-insulator (SOI)”, Opt. Express **3**, 4 (1998).
16. Y. Pennec, B. Djafari-Rouhani, A. Akjouj, J. O. Vasseur, L. Dobrzynski, J. P. Vilcot, M. Beaugeois, M. Bouazaoui, R. Fikri, and J. P. Vigneron, “Transmission filtering of a waveguide coupled to a stub microresonator “, Appl. Phys. Lett. **89**, 101113 (2006).
17. F.-C. Hsu, C.-I. Lee, J.-C. Hsu, T.-C. Huang, C.-H. Wang, and P. Chang, “Acoustic band gaps in phononic crystal strip waveguides”, Appl. Phys. Lett. **96**, 051902 (2010).
18. M. Maldovan and E.L. Thomas, “Simultaneous localization of photons and phonons in two-dimensional periodic structures”, Appl. Phys. Lett. **88**, 251907 (2006).
19. M. Maldovan and E.L. Thomas, “Simultaneous complete elastic and electromagnetic band gaps in periodic structures”, Appl. Phys. B. **83**, 595 (2006).
20. S. Sadat-Saleh, S. Benchabane, F.I. Baida, M.P. Bernal and V. Laude, “Tailoring simultaneous photonic and phononic band gaps”, J. Appl. Phys. **106**, 074912 (2009).

21. D. Bria, M. B. Assouar, M. Oudich, Y. Pennec, J. Vasseur, and B. Djafari-Rouhani, « Opening of simultaneous photonic and phononic band gap in two-dimensional square lattice periodic structure", J. Appl. Phys. **109**, 014507 (2011)
22. S. Mohammadi, A. A. Eftekhar, A. Khelif, and A. Adibi, Opt. Express **18**, 9164 (2010).
23. Y. Pennec, B. Djafari-Rouhani, E. H. El Boudouti, C. Li, Y. El Hassouani, J. O. Vasseur, N. Papanikolaou, S. Benchabane, V. Laude, and A. Martinez, Opt. Express **18**, 14301 (2010).
24. Y. El Hassouani, C. Li, Y. Pennec, E. H. El Boudouti, H. Larabi, A. Akjouj, O. Bou Matar, V. Laude, N. Papanikolaou, A. Martinez, and B. Djafari Rouhani, Phys. Rev. B, **82**, 155405 (2010).
25. AH Safavi-Naeini, O. Painter, "Design of optomechanical cavities and waveguides on a simultaneous bandgap phononic-photonic crystal slab", Opt. Express **18**, 14926 (2010).
26. V. Laude, J.C. Beugnot, S. Benchabane, Y. Pennec, B. Djafari-Rouhani, N. Papanikolaou, J.M. Escalante, A. Martinez, "Simultaneous guidance of slow photons and slow acoustic phonons in silicon phoxonic crystal slabs", Opt. Express **19**, 9690 (2011).
27. Y. Pennec, B. Djafari Rouhani, E. H. El Boudouti, C. Li, Y. El Hassouani, J. O. Vasseur, N. Papanikolaou, S. Benchabane, V. Laude, and A. Martinez, 'Band Gaps and Waveguiding in Phoxonic Silicon Crystal Slabs', Chinese Journal of Phys. **49**, 100.
28. E. Gavartin, R. Braive, I. Sagnes, O. Arcizet, A. Beveratos, T. J. Kippenberg, , "Optomechanical Coupling in a Two-Dimensional Photonic Crystal Defect Cavity", Phys. Rev. Lett. **106**, 203902 (2011).
29. D. A. Fuhrmann, S. M. Thon, H. Kim, D. Bouwmeester, P. M. Petroff, Nature Photonics, doi:10.1038/nphoton.2011.208.
30. M. Eichenfield, J. Chan, R. M. Camacho, K. J. Vahala, and O. Painter, "Optomechanical crystals", Nature **462**, 78 (2009).
31. M. Eichenfield, J. Chan, A.H. Safavi-Naeini, K.J. Vahala, O. Painter "Modeling dispersive coupling and losses of localized optical and mechanical modes in optomechanical crystals", Opt. Express **17**, 20078 (2009).